Identification of the Atomic Structure of the Fivefold Surface of an Icosahedral Al-Pd-Mn Quasicrystal: Helium Diffraction and Scanning Tunneling Microscopy Studies

L. Barbier,[1,*] D. Le Floc'h,[1] Y. Calvayrac,[2] and D. Gratias[3,†]

[1]*Service de Physique et Chimie des Surfaces et Interfaces, CEA/Saclay/DSM/DRECAM, F-91191 Gif-sur-Yvette, France*

[2]*Centre d'études de Chimie Métallurgiques, CNRS, F-94407 Vitry Cedex, France*

[3]*Laboratoire d'étude des Microstructures, CNRS/ONERA, F-92322 Châtillon Cedex, France*

(Received 3 August 2001; published 11 February 2002)

High resolution He diffraction and scanning tunneling microscopy images of the fivefold surface of a single-grain i-AlPdMn quasicrystal are obtained showing an almost perfect quasicrystal order. Observed configurations can be identified within the framework of polyhedral models. The terrace terminations are found to be Al-rich planes and successions of step heights agree with distances between dense Al planes in the model. This shows the ability of recent 6D polyhedral models to describe real quasicrystalline atomic configurations.

DOI: 10.1103/PhysRevLett.88.085506 PACS numbers: 61.44.Br, 61.50.Ah, 68.35.Bs

Quasicrystals (QCs) are fascinating solids exhibiting long range orientational order inconsistent with crystal periodicity. More than 15 years after their discovery [1], their bulk atomic structures can globally be described as relatively compact quasiperiodic stacking of atoms (or clusters of atoms), in which typical structural defects (called phasons) develop according to a physics that is still subject to discussion. As for the usual crystals, most of our knowledge of the atomic structures of QCs is extracted from diffraction experiments of bulk single-grain samples and high resolution electron microscopy (HREM) performed on thin foils (see, for instance, Ref. [2]). In both cases, the interpretation of the experimental results are based on the "ideal QC model" that is the quasicrystalline analog of the "ideal crystal model." All these models fit the experimental data to an accuracy that is comparable to the one achieved in crystals *before* processing the usual crystallographic refinement (Debye-Waller corrections, atomic position adjustments, etc.). Comparison in direct space of the models against the actual structures are best achieved using HREM images that are still 2D projections of the bulk structures. Surface studies, on the contrary, lead to valuable structural information with no effect of thickness averaging, leading thus to a direct comparison between models and experiments. We present here a high resolution scanning tunneling microscopy (STM) investigation of flat terraces on fivefold atomic planes of icosahedral AlPdMn QC that has a sufficient resolution for being unambiguously understood in terms of the specific structural features of the bulk material, as expected from ideal QC models. It is found that the terraces correspond to exact cuts (with possible unobservable relaxations) of the bulk material across the basic atomic clusters of the structure, so-called pseudo-Bergman (B) and pseudo-Mackay (M) clusters. The high quality of the investigated QC, together with the high performance of modern STM and the recent development of 6D polyhedral structural models allowed us to reach this aim.

Surface structures of QCs have been intensively investigated during these past years by means of various surface characterization tools (see, for instance, Ref. [3]). Among the many problems posed by QCs is the experimental characterization of the termination plane of the bulk materials which has been investigated by means of high resolution scanning tunneling microscopy imaging [4–7]. So far, the achieved resolution of STM images clearly showed flat terraces with fivefold quasiperiodicity but did not allow us to unambiguously relate these geometric features with the actual atomic structure of the bulk material because of an insufficient resolution (except notably in the case of the $Al_{65}Co_{20}Cu_{15}$ decagonal QC [8]) and of the relatively high density of local defects.

A large centimeter sized single-grain QC of i-AlPdMn has been obtained by the Czochralsky method of slow extraction from the liquid through an incongruent solidification [9]. The QC exhibits well-developed large facets at the solid-liquid interface that are rather unusual in metallic alloy single-grain growths. The composition, measured by plasma optical emission spectroscopy at different locations, is $Al_{71.1}Pd_{20.2}Mn_{8.7}$. X-ray powder diffraction of fragments of the QC confirms the expected F-type icosahedral structure as a single phase of the material. 2-mm-thick slabs are cut by electroerosion parallel to the natural facets that are perpendicular to fivefold directions, as determined by Laue diffraction.

In order to remove the native oxide layer, one as-grown facet of the sample has been softly polished mechanically before being introduced into the ultrahigh vacuum STM chamber. There, a standard cleaning process (cycles of 5 μA, 400 V, 1 h Ar^+ sputtering, and 925 K, 1 h annealing) was used and monitored by Auger electron spectroscopy (AES) and low energy electron diffraction (LEED).

AES measurements show a preferential Al sputtering, indicating a high Al concentration within the surface plane. Annealing allows one to restore the surface composition with a relative intensity of the AES peaks: Al(68 eV)/Pd(330 eV) = 1 and Mn(40 eV)/Pd(330 eV) = 0.3. After Ar^+ sputtering the LEED pattern presents fivefold diffuse spots. Upon annealing the spots become sharper and more intense. No evidence is found for the often-reported tenfold pattern [10]. In order to reach the best possible surface state, He diffraction was eventually used before STM observations. As a technique sensitive only to the very outermost surface plane, He diffraction (K_i = 65 nm^{-1}) is an excellent tool to characterize the whole surface on the atomic scale. The He diffraction pattern shows a narrow and intense (up to 6% of the incident beam) specular peak (see Fig. 1) surrounded by a fivefold set of diffraction peaks of low intensity ($I_G \sim 1.5\%$ of the specular intensity). In the incidence plane, the positions of successive diffraction peaks follow a τ scale: $\Delta K_G = \tau^{G-1}\Delta K_1$, where $\Delta K_1 = 2\pi/a$, $a = 1.7 \pm 0.1$ nm. Since the diffraction peak intensities I_G are weak with respect to the specular intensity I_0, the kinematic (or eikonal) approximation can be used to obtain the amplitude A_c of the fivefold Fourier component of the surface corrugation, according to

$$A_c = \frac{1}{K_{Gz} - K_{0z}} \sqrt{\frac{I_G K_{0z}}{I_0 K_{Gz}}},$$

where K_{Gz} and K_{0z} are the perpendicular components to the surface of the wave vector. One obtains $A_c = 1.92$ pm. With respect to the incident angle, the specular peak intensity varies slowly with a constant width slightly larger than the instrumental resolution (0.35°), giving a terrace size of the order of 45 nm. We conclude that the whole surface is uniformly made of wide, very flat, terraces with a low fivefold corrugation of the He surface potential. During the experiment, successive surface cleaning cycles (more than 100) made the He diffraction pattern more intense, thus indicating an excellent stability of the surface. In that way, this experiment allowed optimizing annealing temperature and time to get the maximum diffraction intensities and, correlatively, the best surface state.

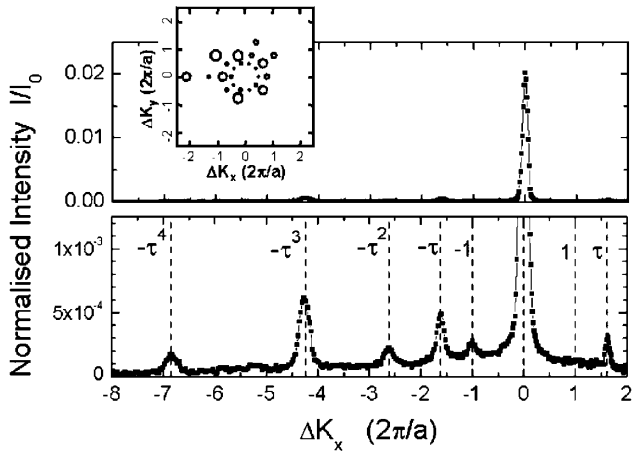

FIG. 1. Typical He diffraction spectrum (wave number of the incident beam: K_i = 65 nm^{-1}, incidence angle: $i = 58°$, a = 1.7 nm), ΔK_x designates the momentum transfer within the incident plane. Top: normalized intensity (not corrected for Debye-Waller attenuation). Bottom: intensity scale (×20). Diffraction peaks are observed up to the 5th order. Inset: fivefold diffraction pattern. Circles are proportional to peak intensities.

In agreement with the former He diffraction study, STM investigations reveal wide flat terraces (40 nm) bounded by steps, as shown by the STM image in Fig. 2. Steps of the most frequent heights are 0.68 (h_0), 0.42, and 0.26 nm edge terraces. Other heights can be found and scale according to h_0/τ^n, n being a positive or negative integer number. Steps meander and one step of height h can split in (or be the combination of) two individual steps of respective heights h/τ and $h(1 - 1/\tau) = h/\tau^2$. Figure 3(a) shows a typical high resolution STM image (18.5 × 16 nm^2, corrugation 0.04 nm) of the fivefold surface obtained within one of these terraces. The intensity spectrum of the image (inset) shows several orders of sharp peaks evidencing a high quality quasiperiodic fivefold symmetry surface structure. Peak intensities give an amplitude of the fivefold Fourier component of the surface corrugation of 2.8 pm. One can note that STM and He diffraction see nearly the same isoelectronic surface. The image shows locally pentagonal "flowers" of "donutlike" patterns [see Figs. 3(b) and 3(c)] that distribute along well-defined rows. Individual flowers are not strictly fivefold. The intensity of each petal is not uniform, thus revealing a complex electronic distribution. Flowers overlap and distribute equally according to two up and down orientations.

One main difficulty to interpret these types of real images of QCs at the atomic scale comes from their aperiodicity. Most of the many remarkable geometric properties observed so far on STM images (fragments of Fibonacci-like sequences of parallel lines along aligned dots and/or drawing inflated pentagons of these dots [4,8,11]) directly result from the basic properties of quasiperiodicity and are shared by all QCs of the same local isomorphism class. Deciphering the STM images with respect to their atomic structure requires analyzing local configurations as

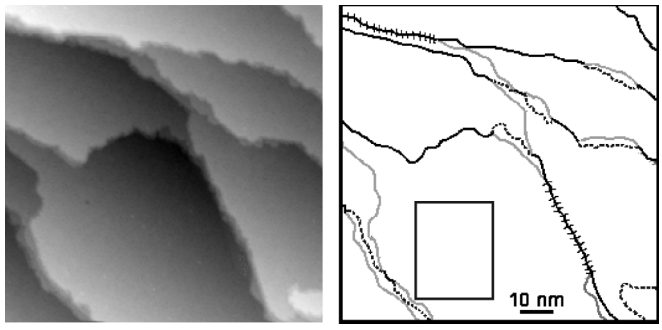

FIG. 2. Left: STM image (93 × 93 nm^2) showing the terrace and step structure. Right: step heights: (—) h_0 = 0.68 nm; (grey line) h_0/τ; (− − −) h_0/τ^2; (++++) $h_0(1 + 1/\tau)$. Rectangle: approximate location of the STM image of Fig. 3.

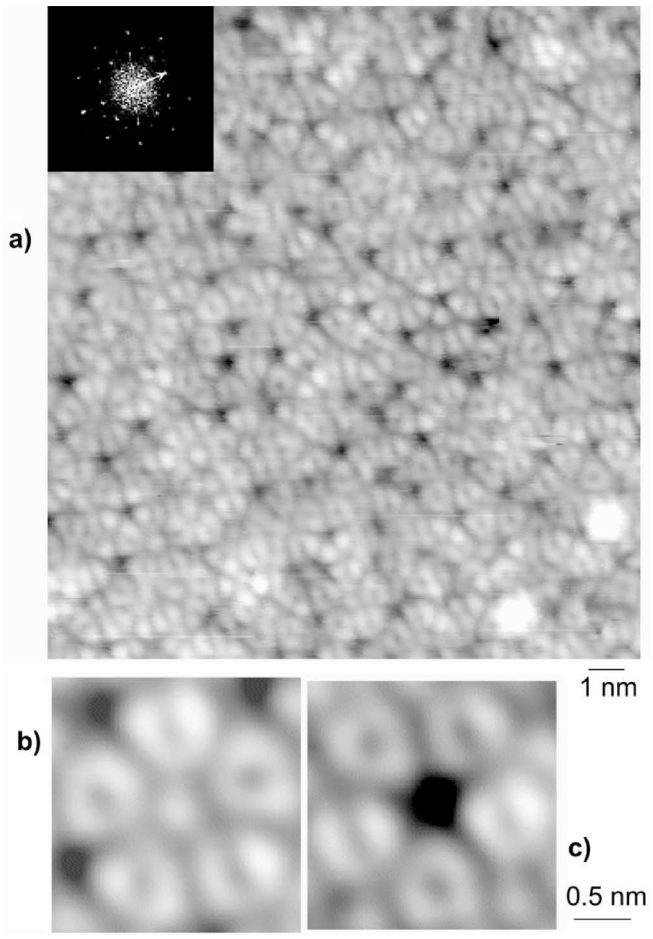

FIG. 3. (a) High resolution STM image (18.5 × 16 nm^2, I = 2.5 nA, $V = -0.35$ V) of a fivefold terrace of i-AlPdMn. Inset: intensity spectrum of the Fourier transform of the image (white arrow, 2 nm^{-1}). (b),(c) The two types of pentagonal flowers (2.2 × 2.2 nm^2) that are well-recognizable local patterns of the image. In (a), all "up-flower"–like patterns (b) have a filled center and all "down-flower" patterns (c) have a hollow center.

a function of the way they appear in space. As a property of QC structures, any local pattern of a given size repeats identically in the structure. Increasing the size of the selected area makes its repetition less frequent and more difficult to interpret. Limiting ourselves to local configurations (whose size can be extended at the price of computing a QC model of a larger size) would allow analyzing them from the following model.

To achieve this goal, we choose to interpret the STM images on the basis of the six-dimensional hyperspace representation [12–17] of the F-type icosahedral structures. In that scheme, i-AlPdMn is described as a 3D cut of a 6D periodic crystal with a face-centered (F) hypercubic lattice properly oriented to reflect the icosahedral symmetry. Atoms are defined by 3D volumes, the so-called atomic surfaces (AS), embedded in the 3D space perpendicular to the physical 3D space. They are polyhedra periodically distributed on special points of the 6D lattice [17]. Their traces in the 3D real space are points that define the locations of the atoms in the actual QC. The local atomic configurations can therefore be analyzed by studying how neighboring AS's simultaneously intersect the physical space (or, equivalently, overlap in perpendicular space). In our model, the atomic decoration has been recently adjusted so as to reproduce x-ray and very recent complementary neutron diffraction data [18], together with magnetic properties indicating that Mn atoms must be uniformly distributed on the lattice at an average distance of 0.48 nm from each other. As a result, three main atomic surfaces fitting together are necessary to fill the structure. The 3D structure can also be described in terms of atomic clusters in the spirit introduced by Kasner *et al.* [16] in their pioneering attempt to connect STM images with quasiperiodic tiling descriptions. Recent detailed analyses [17–25] of the various models of the bulk F-type icosahedral AlCuFe and AlPdMn structures show that roughly 80% (depending slightly on the model) of the atoms can be described as a network of 33 atom clusters (one Pd atom at the center, 12 Al on an inner icosahedron, and 20 atoms, a mixture of roughly 12 Al, 8 Pd, and some fractions of Mn, on an external dodecahedron). These clusters, designated as B clusters (pseudo-Bergman), are connected by edges and located at the even nodes of a simple 3D Penrose tiling. Quandt and Elser [25] recently showed, by density functional minimization of an initially disordered icosahedral QC, a tendency to form such B clusters. Overlapping this basic skeleton, two closely related types of clusters of 50 atoms, called M and M' clusters (pseudo-Mackay), can be alternately defined and contain space fillers and numerous atoms of the B clusters themselves. All configurations around these M and M' clusters have at least one pentagon of surrounding B clusters. These pentagonal configurations of B clusters are the most frequent configurations encountered in the fivefold planes.

Using the above polyhedral model, a 10 nm diameter bowl of the QC has been computed containing roughly 35 000 atoms. The atoms distribute on well-defined planes perpendicular to each fivefold axis. Cutting the bowl along these planes, one could compare the atomic structure with STM observed configurations. For easier comparison to STM images, electronic density maps can be generated from the simple superposition of exponentially decaying electronic densities centered on atoms. Some planes contain very few atoms and can be discarded. Some others are dense planes. Among them, one configuration [see Fig. 4(b)] of more than 8 nm diameter matches nearly exactly the observed STM structure [see Fig. 4(a)]. The matching plane is, in the model, a pure Al plane in agreement with the Auger analysis that indicates an Al-rich surface composition. In addition, the larger scale image in Fig. 2 of the same area allows measuring the height of the steps edging the considered terrace and of the next steps. The observed succession of step heights is identical to the succession of Al-rich dense planes in the model, except for the upper terrace. Undoubtedly, one other sequence, fully compatible with the observed one, could be found in a larger bowl. Correlation of the selected area [Fig. 4(a)]

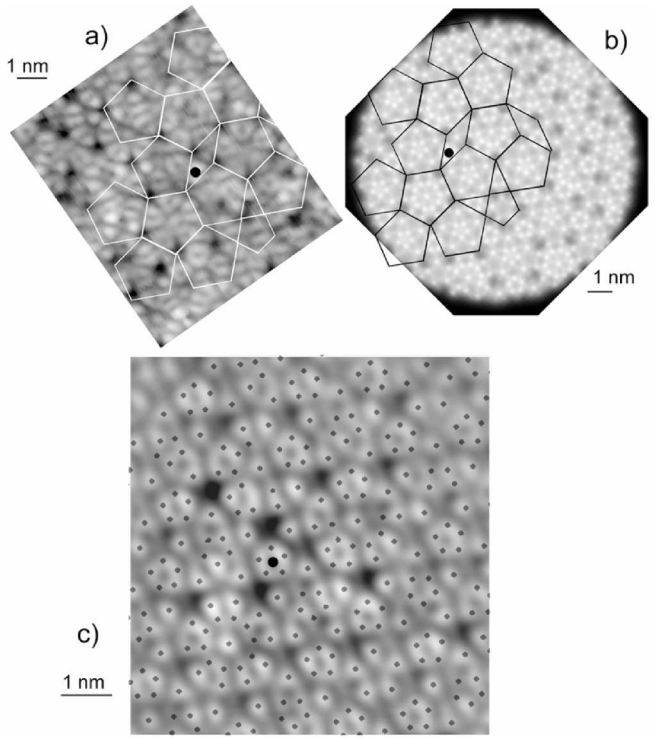

FIG. 4. (a) (7.8×8.8 nm^2) STM image. (b) Simulated STM image (10 nm diameter) from the Katz-Gratias structural model [18,21]; the exponential decay parameter of electronic densities and the observation distance are chosen for single surface atoms. A geometrical pattern joining black holes and a black dot is drawn to guide the eye. Between (a) and (b), distributions of black holes are very close. (c) STM average image of identical configurations selected by correlation of the selected area (a) with the entire image. Dots: positions of Al atoms according to the model. Minute details of the experimental image are in agreement with the Al atomic distribution.

with the entire image (Fig. 3) allows finding very similar configurations. Averaging them allows the elimination of the STM noise and casual point defects. The Al atom distribution of the model perfectly reproduces minute details of the resulting image [Fig. 4(c)]. Note that the "donut" patterns that are not round can be explained by the various number of Al atoms (3, 4, or 5) within one donut in the model surface plane. This allows, for the first time, to unambiguously interpret STM images made of dense (almost) pure Al atomic planes, where the atoms distribute according to our polyhedral model. This surface plane truncates both B and M (M') clusters. This makes questionable the stability of these clusters to interpret the stability of QCs (and QC surfaces) and their ability to carry the local matching rules expected for propagating long range QC order. On the reverse, our result confirms the validity of the polyhedral 6D approach to describe QC structures at atomic scale. Note that wider configurations, not discussed here, can be described as the effort of generating from the models the large, but finite, sets of possible extended configurations.

The ability of 6D polyhedral models to interpret STM images opens the door to the identification of defects. Answers to fundamental questions about QC growth, stability, and long range and short range QC order could be found in that way.

The authors acknowledge fruitful discussions with M. Quiquandon, L. Bresson (ONERA), and F. Charra (CEA) in the interpretation of the images. The technical support of P. Lavie and F. Merlet (CEA) was essential for both He and STM experiments.

*Electronic address: lbarbier@cea.fr
†Electronic address: gratias@onera.fr

[1] D. Shechtman, I. Blech, D. Gratias, and J.-W. Cahn, Phys. Rev. Lett. **53**, 1951 (1984).
[2] See, for instance, K. Hiraga, in *Quasicrystals: The State of the Art,* edited by D. P. Divicenzo and P.-J. Steinhardt (World Scientific, Singapore, 1991).
[3] See, for instance, J. Chevrier, in *Quasicrystals: Current Topics,* edited by E. Belin-Ferré, C. Berger, M. Quiquandon, and A. Sadoc (World Scientific, Singapore, 2000).
[4] T. M. Schaub, D. E. Bürgler, H.-J. Güntherodt, and J. B. Suck, Phys. Rev. Lett. **73**, 1255 (1994).
[5] D. Rouxel *et al.,* Surf. Sci. **461**, L521 (2000).
[6] Z. Shen, C. R. Stoldt, C. J. Jenks, T. A. Lograsso, and P. A. Thiel, Phys. Rev. B **60**, 14 688 (1999).
[7] J. Ledieu *et al.,* Surf. Sci. **433–435**, 666 (1999).
[8] A. R. Kortan, R. S. Becker, F. A. Thiel, and H. S. Chen, Phys. Rev. Lett. **64**, 200 (1990).
[9] Y. Yokohama, T. Miura, A. Tsai, A. Inoue, and T. Masumoto, Mater. Trans. JIM **33**, 97 (1992).
[10] F. Schmithüsen *et al.,* Surf. Sci. **444**, 113 (2000).
[11] J. Ledieu *et al.,* Surf. Sci. Lett. **492**, L729 (2001).
[12] A. Katz and M. Duneau, J. Phys. (Paris) **47**, 181 (1986).
[13] V. Elser, Acta Crystallogr. Sect. A **42**, 36 (1986).
[14] P. A. Kalugin, A. Y. Kitayev, and L. S. Levitov, JETP Lett. **41**, 145 (1985).
[15] J. W. Cahn, D. Gratias, and B. Mozer, Phys. Rev. B **38**, 1638 (1988).
[16] G. Kasner, Z. Papadopolos, P. Kramer, and D. E. Bürgler, Phys. Rev. B **60**, 3899 (1999).
[17] D. Gratias, F. Puyraimond, M. Quiquandon, and A. Katz, Phys. Rev. B **63**, 24 202 (2001).
[18] N. Shramchenko, R. Caudron, R. Bellissent, and D. Gratias (to be published); N. Shramchenko, Ph.D. thesis, Université Paris XI Orsay, 2001.
[19] M. Cornier-Quiquandon *et al.,* Phys. Rev. B **44**, 2071 (1991).
[20] M. Boudard *et al.,* J. Phys. Condens. Matter **4**, 10 149 (1992).
[21] A. Katz and D. Gratias, J. Non-Cryst. Solids **153–154**, 187 (1993); in *Proceedings of the 5th International Conference on Quasicrystals,* edited by C. Jannot and R. Mosseri (World Scientific, Singapore, 1995).
[22] E. Cockayne *et al.,* J. Non-Cryst. Solids **153–154**, 140 (1993).
[23] V. Elser, Philos. Mag. B **73**, 641 (1996).
[24] Z. Papadopolos, P. Kramer, and W. Liebermeister, in *Proceedings of the 6th International Conference on Quasicrystals 1997,* edited by S. Takeuchi and T. Fujiwara (World Scientific, Singapore, 1998).
[25] A. Quandt and V. Elser, Phys. Rev. B **61**, 9336 (2000).